THE JOURNAL OF BIOLOGICAL CHEMISTRY VOL. 291, NO. 35, pp. 18299–18308, August 26, 2016

Protein Arginine Methyltransferase Product Specificity Is Mediated by Distinct Active-site Architectures*

Received for publication, June 1, 2016, and in revised form, July 5, 2016 Published, JBC Papers in Press, July 7, 2016, DOI 10.1074/jbc.M116.740399

Kanishk Jain[‡], Rebeccah A. Warmack[‡], Erik W. Debler[§1], Andrea Hadjikyriacou[‡], Peter Stavropoulos[§¶], and Steven G. Clarke[‡2]

From the [‡]Department of Chemistry and Biochemistry and the Molecular Biology Institute, UCLA, Los Angeles, California 90095 and the [§]Laboratory of Cell Biology and [¶]Laboratory of Lymphocyte Biology, The Rockefeller University, New York, New York 10065

In the family of protein arginine methyltransferases (PRMTs) that predominantly generate either asymmetric or symmetric dimethylarginine (SDMA), PRMT7 is unique in producing solely monomethylarginine (MMA) products. The type of methylation on histones and other proteins dictates changes in gene expression, and numerous studies have linked altered profiles of methyl marks with disease phenotypes. Given the importance of specific inhibitor development, it is crucial to understand the mechanisms by which PRMT product specificity is conferred. We have focused our attention on active-site residues of PRMT7 from the protozoan *Trypanosoma brucei*. We have designed 26 single and double mutations in the active site, including residues in the Glu-Xaa$_8$-Glu (double E) loop and the Met-Gln-Trp sequence of the canonical Thr-His-Trp (THW) loop known to interact with the methyl-accepting substrate arginine. Analysis of the reaction products by high resolution cation exchange chromatography combined with the knowledge of PRMT crystal structures suggests a model where the size of two distinct subregions in the active site determines PRMT7 product specificity. A dual mutation of Glu-181 to Asp in the double E loop and Gln-329 to Ala in the canonical THW loop enables the enzyme to produce SDMA. Consistent with our model, the mutation of Cys-431 to His in the THW loop of human PRMT9 shifts its product specificity from SDMA toward MMA. Together with previous results, these findings provide a structural basis and a general model for product specificity in PRMTs, which will be useful for the rational design of specific PRMT inhibitors.

Methylation of proteins is a major type of post-translational modification involved in the regulation of a variety of cellular processes mediated by protein-protein interactions, including splicing, transcription, translation, and signaling (1–3). Recent studies have implicated arginine methylation in altering the metabolic landscape of the cell, linking it to cancer metastasis (4–6), DNA damage (7), pluripotency (8), and parasite infection (9, 10). Catalysis of arginine methylation on the terminal nitrogen atoms of the guanidine group is mediated by a family of enzymes designated as protein arginine methyltransferases (PRMTs).[3] Most of these enzymes harbor a conserved ~310-residue core that comprises the methyltransferase domain conserved in *S*-adenosylmethionine (AdoMet)-dependent methyltransferases and a β-barrel domain unique to the PRMT family. These enzymes can be further categorized based on which methylarginine product they catalyze as follows: type I PRMTs catalyze the production of ω-N^G-monomethylarginine (MMA) and asymmetric ω-N^G,N^G-dimethylarginine (ADMA); type II PRMTs catalyze the production of MMA and symmetric ω-N^G,N'^G-dimethylarginine (SDMA); type III PRMTs catalyze the production of only MMA; and type IV PRMTs catalyze δ-N^G-monomethylarginine production (11). Notably, most PRMTs fall under the first three types of PRMTs. Type IV enzymes have only been reported in yeast and plants, although the presence of free δ-N^G-monomethylarginine has been reported in human plasma in a recent proteomic study (12).

ADMA and SDMA methyl marks on histones are recognized by different "reader" proteins and can lead to distinct downstream outcomes. For example, whether a particular arginine residue on histone tails is asymmetrically or symmetrically dimethylated can lead to gene repression or activation (13–17). However, few studies have been conducted to determine the role of MMA marks (18). It has been proposed that MMA marks are used mainly as precursors for dimethylation by the various type I and II PRMTs (17, 19).

Given the biological significance of the type of methylated arginine derivative formed, it is important to understand how product specificity is determined in PRMTs. It has been suggested that small variations in the structure of the active site of these enzymes govern the methylation activity type (2, 3, 20–23). Although previous studies utilizing site-directed mutagenesis have given some support for this hypothesis, efforts to efficiently change the activity type of PRMTs have not yet been fruitful. Two such studies using moderately sensitive analytical techniques have been reported for PRMT1 (14) and

* This work was supported by National Institutes of Health Grant GM026020 (to S. G. C.) and Ruth L. Kirschstein National Service Award GM007185 (to K. J., R .A. W., and A. H.). The authors declare that they have no conflicts of interest with the contents of this article. The content is solely the responsibility of the authors and does not necessarily represent the official views of the National Institutes of Health.

[1] Frey Fellow of the Damon Runyon Cancer Research Foundation supported by Grant DRG-1977-08.

[2] To whom correspondence should be addressed: Dept. of Chemistry and Biochemistry and Molecular Biology Institute, UCLA, 607 Charles E. Young Dr. East, Los Angeles, CA 90095. Tel.: 310-825-8754; E-mail: clarke@mbi.ucla.edu.

[3] The abbreviations used are: PRMT, protein arginine methyltransferase; MMA, ω-N^G-monomethylarginine; ADMA, ω-N^G,N^G-asymmetric dimethylarginine; SDMA, ω-N^G,N'^G-symmetric dimethylarginine; AdoHcy, *S*-adenosyl-L-homocysteine; AdoMet, *S*-adenosyl-L-methionine; [*methyl*-^{3}H]-AdoMet, *S*-adenosyl-[*methyl*-^{3}H]-L-methionine; ITC, isothermal titration calorimetry.

TABLE 1

Product analyses of wild-type and mutant *Tb*PRMT7 enzymes with the H4(1–21) R3MMA peptide

The number of experiments is indicated in parenthesis. As shown under the "Experimental Procedures," 86 cpm correspond to 1 fmol of methyl groups.

	[^{3}H]Methyl group radioactivity in MMA (average cpm)	[^{3}H]Methyl group radioactivity in ADMA (average cpm)	[^{3}H]Methyl group radioactivity in SDMA (average cpm)
***Tb*PRMT7 enzyme**			
Wild type (n = 4)	11,093	0	0
Automethylation (n = 4)	122	0	0
Double E loop mutants			
G180N (n = 1)	6,648	0	0
G180Y (n = 1)	5,365	0	0
E172Q (n = 1)	0	0	0
E181D (n = 3)	294	161	0
E181Q (n = 1)	62	0	0
I173G (n = 1)	0	0	0
I173A (n = 1)	121	0	0
I173V (n = 1)	7,231	0	0
I173P F174 M (n = 1)	0	0	0
I173L F174L (n = 1)	29,487	0	0
G175D M177E (n = 1)	0	0	0
E172D E181D (n = 1)	0	0	0
E181D I173G (n = 2)	64	0	0
THW loop mutants			
Q329A (n = 1)	420	0	0
Q329F (n = 1)	95	0	0
Q329H (n = 1)	23,218	0	0
W330A (n = 1)	437	0	0
Q329N (n = 1)	3,322	0	0
Helix αY mutants			
F71A (n = 1)	123	0	0
M75A (n = 1)	205	0	0
M75F (n = 1)	644	0	0
Double E loop and THW loop double mutants			
E181D W330A (n = 1)	52	0	0
E181D Q329A (n = 2)	89	0	500
E181D Q329N (n = 1)	0	0	0
Double E loop and helix αY double mutants			
E181D M75A (n = 1)	65	0	0
E181D F71A (n = 1)	143	0	0

PRMT5 (24), but they have not put forth a general model for the factors that guide product specificity for the three main types of PRMTs.

Using an approach where MMA, ADMA, and SDMA can be detected with sub-femtomole sensitivity, we have been able to demonstrate the transformation of PRMT7 from *Trypanosoma brucei* (*Tb*PRMT7) from an enzyme that strictly produces MMA to one also forming ADMA by replacing a glutamate residue in the double E loop (Glu-181) with an aspartate residue (Fig. 1) (25). The double E loop is a conserved feature of PRMTs that has been shown to directly interact with the methyl-accepting arginine residue (2, 11). *Tb*PRMT7 had been initially characterized for a possible role in the transcriptional control of gene expression in this organism (26). Here, we have focused on *Tb*PRMT7 because it displays robust type III activity and has been amenable to structural analysis (25–27). Within this work, we further examine the effects of key active-site residues on the enzymatic activity of *Tb*PRMT7 through mutagenesis and highly sensitive amino acid analysis techniques to demonstrate the importance of the THW loop (MQW for *Tb*PRMT7) (Fig. 1) (2). Complementary studies with PRMT9 from *Homo sapiens*, previously characterized as a type II enzyme (28, 29), corroborate our PRMT7 results. Based on this evidence, we propose a structural model for how PRMTs can limit their activities to type I, type II, or type III methylation.

Results

TbPRMT7 Active-site Double Mutation, E181D/Q329A, Converts the Enzyme to an SDMA-producing PRMT—Given the ability of the double E loop E181D mutation of *Tb*PRMT7 to alter the methylation type (25), seven *Tb*PRMT7 double mutants were generated with the E181D background to probe the effects of further increasing the size of the active site. Notably, the double mutant E172D/E181D was previously tested and found inactive (Table 1) (25). The additional substitutions in the six new double mutants included M75A, Q329A, Q329N, W330A, F71A, and I173G, each with the E181D mutation, based on their immediate vicinity to the sulfur atom of AdoHcy from which the methyl group of AdoMet is transferred to the arginine residue in protein and peptide substrates (Fig. 1). Using [*methyl*-^{3}H]AdoMet as a cofactor, we analyzed the hydrolyzed products of arginine methylation with high resolution cation exchange chromatography. Two of these double mutants showed little or no activity toward either the H4(1–21) peptide, comprised of the acetylated 21 N-terminal residues of the human histone H4 protein (data not shown), or the acetylated H4(1–21) R3MMA peptide, ω-monomethylated at the third arginine (Table 1). The H4(1–21) R3MMA peptide was used to enhance the detection of dimethylarginine derivatives by providing a substrate where a single methyla-

tion reaction at the primary site of modification could result in dimethylation of the peptide. Strikingly, one of the double mutants, E181D/Q329A, produced SDMA when incubated with the H4(1–21) R3MMA peptide (Fig. 2, *A* and *B*). The small amount of MMA produced in the reaction of the E181D/Q329A mutant with the H4(1–21) R3MMA peptide is most likely due to methylation of the secondary Arg-17 and Arg-19 sites on the histone peptide because the level of radioactivity here is higher than the level recorded for the enzyme alone (Fig. 2*B*). Importantly, although this enzyme contains the ADMA-producing mutation E181D (25), as well as a Q329A mutation in the THW loop, no ADMA formation was detected. SDMA production catalyzed by the E181D/Q329A mutant was confirmed by TLC analysis where the radioactive product co-migrated with the non-radioactive SDMA standard (Fig. 2*C*). The wild-type *Tb*PRMT7 does not produce any dimethylarginine products with either H4(1–21) or H4(1–21) R3MMA peptide (Fig. 3). The single Q329A mutant shows no evidence of dimethylarginine formation (Table 1).

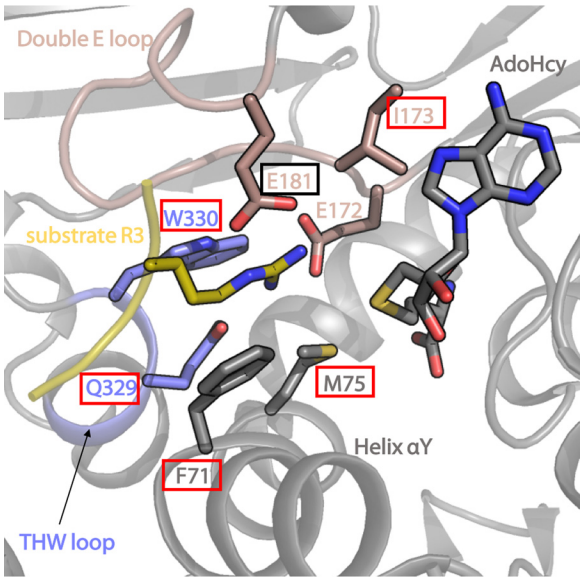

FIGURE 1. **Active site of *T. brucei* PRMT7.** Residue Glu-181, highlighted in the *black box*, is the site of mutation (E181D) shared by the six double mutants in this study with their second mutated residue highlighted in a *red box* (W330A, Q329A, Q329N, F71A, M75A, and I173G). The double mutant E172D/E181D was previously analyzed and Glu-172 is therefore not highlighted here (25). The double E loop is shown in *dark salmon*, the THW loop in *slate*, the substrate arginine residue in *yellow*, and the AdoHcy cofactor, helix αY, and adjacent residues of *Tb*PRMT7 (Protein Data Bank code 4M38) in *gray*.

TbPRMT7 Shows Higher Binding Affinity for the Monomethylated Histone H4(1–21) Peptide Than for the Unmethylated Peptide—Using isothermal titration calorimetry (ITC) with H4(1–21) and H4(1–21) R3MMA peptides, we previously demonstrated that the wild-type *Tb*PRMT7 enzyme binds its substrate H4(1–21) with higher affinity than its monomethylated product, H4(1–21) R3MMA, whereas the ADMA-producing *Tb*PRMT7 E181D mutant has markedly increased affinity for H4(1–21) R3MMA that even surpasses that for H4(1–21) (25). Similarly, we measured the affinity of the SDMA-producing *Tb*PRMT7 E181D/Q329A enzyme and

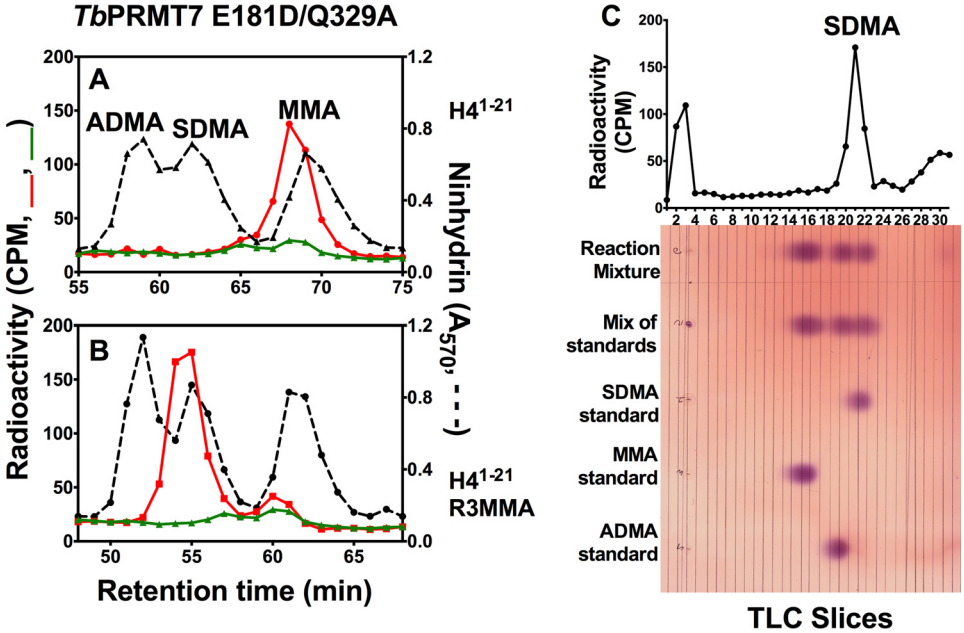

FIGURE 2. ***Tb*PRMT7 E181D/Q329A double mutant produces SDMA with the H4(1–21) R3MMA peptide.** The specificity of this mutant was determined using cation exchange chromatography and TLC as described under "Experimental Procedures." *Tb*PRMT7 E181D/Q329A (4.8 μg of protein) was incubated with the H4(1–21) or H4(1–21) R3MMA peptide (10 μM) and [*methyl*-^{3}H]AdoMet in a final volume of 60 μl. *A, Tb*PRMT7 E181D/Q329A double mutant with the H4(1–21) peptide. *B, Tb*PRMT7 E181D/Q329A with the H4(1–21) R3MMA peptide. The *red lines* in *A* and *B* represent radioactivity of the E181D/Q329A mutant with the different substrates, and the *green lines* indicate radioactivity of the methylation reaction with no substrate. As noted previously (25), radioactive methylarginine derivatives elute 1 min earlier than their non-radioactive counterparts due to the isotope effect (39, 40). As given under "Experimental Procedures," 86 cpm correspond to 1 fmol of methyl groups. For the number of biological replicates, see Table 1. *C,* representative TLC for hydrolysates of the reaction mixture and individual and mixed standards of ADMA, MMA, and SDMA. The *lower portion* shows the ninhydrin staining of the TLC plate; the *upper portion* shows the radioactivity corresponding to the TLC slices of the reaction mixture lane. Note: the ninhydrin standards on the TLC plate are the same as those shown in Fig. 4*D* of Ref. 25 where a different reaction mixture was chromatographed adjacent to the ADMA standard lane. The experiment is one of two biological replicates.

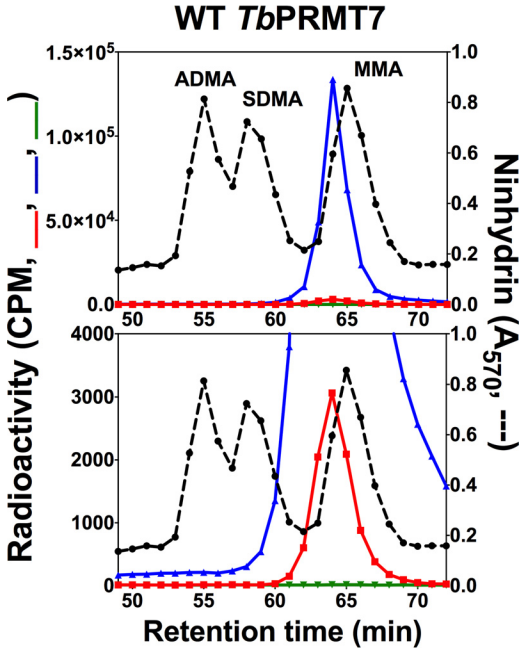

FIGURE 3. **Wild-type *Tb*PRMT7 displays no dimethylarginine production with H4(1–21) and H4(1–21) R3MMA peptides.** *In vitro* methylation and cation exchange chromatography were used as described under "Experimental Procedures" to assess wild-type *Tb*PRMT7 activity and product specificity with H4(1–21) (*blue*), H4(1–21) R3MMA peptides (*red*), or with the enzyme alone (*green*). *Dashed black lines* indicate elution profile of non-radioactive methylarginine species as measured by a ninhydrin assay (see "Experimental Procedures"). The *lower panel* represents enlargement of the radioactivity in the *upper panel* to show low levels of methylation. As given under the "Experimental Procedures," 86 cpm correspond to 1 fmol of methyl groups. For the number of biological replicates, see Table 1.

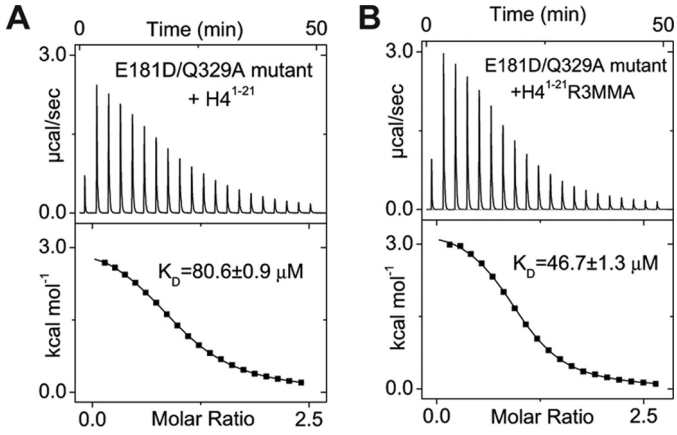

FIGURE 4. **Isothermal titration calorimetry of the *Tb*PRMT7 E181D/Q329A mutant with H4(1–21) (*A*) and H4(1–21) R3MMA (*B*), respectively.** Each titration was performed twice.

found that this mutant displays higher affinity for H4(1–21) R3MMA (K_D = 46.7 μM) *versus* its unmethylated counterpart H4(1–21) (K_D = 80.6 μM) (Fig. 4). Thus, the two mutant enzymes capable of dimethylation consistently favor binding of the bulkier H4(1–21) R3MMA peptide, which can be rationalized by providing a more spacious binding pocket, stabilizing the MMA substrate-enzyme interactions and enabling dimethylation.

Active-site Mutations Lead to Decreases in Type III PRMT7 Activity and Shifts in Recognition Site Specificity—Overall, we have reacted 26 single and double mutants of *Tb*PRMT7 with the H4(1–21) R3MMA peptide to test whether active-site mutations could display changes in the methylation type when presented with a primed monomethylarginine (Table 1). These mutations were generated based on their location in the active site of *Tb*PRMT7, including residues in the double E loop, the AdoMet-binding motif, the THW loop, and an N-terminal extension (helix αY). The majority of the active-site mutations result in decreases in enzyme activity. However, monomethylation is still observed, indicating that the modification of Arg-17 and Arg-19 on the substrate peptide is occurring, as Arg-3 is already methylated in this peptide. This finding suggests that there may be a change in recognition site specificity from glycine-arginine-rich regions to arginine residues in basic regions (26, 30). Notably, the THW (MQW) loop mutant Q329H showed significant increases in MMA production. Most remarkably, the double mutant E181D/Q329A produced both MMA and SDMA, as described above.

Mutation in the THW Loop of Human PRMT9, a Type II PRMT, Shifts Product Specificity from SDMA toward MMA—The human PRMT9 has recently been characterized as a type II PRMT, joining PRMT5 as an enzyme that catalyzes SDMA production (28, 29). This methyltransferase contains a Thr-Cys-Trp (TCW) sequence in place of the canonical Thr-His-Trp (THW) residues (28). To further investigate the role of spatial restrictions conferred by key active-site residues, the cysteine residue was mutated to a bulkier histidine residue to mimic type I and type III PRMTs. These mutant and wild-type enzymes were reacted with a GST fusion of the splicing factor SF3B2, a known substrate of PRMT9 (28). Comparison of wild-type and mutant activities reveals an impressive 8-fold increase in MMA production and almost complete elimination of SDMA production (<0.037%) (Fig. 5).

Rattus norvegicus PRMT1 M48F Mutant Enzyme Does Not Produce SDMA with Histone H4 Peptides—A previous study (24) reported a mutation in rat PRMT1 at Met-48, a residue conserved in the αY helix of many PRMTs, to Phe. This change led to the apparent production of SDMA along with ADMA and MMA, the wild-type products of a type I PRMT, as determined by *o*-phthalaldehyde-derivatized reverse-phase liquid chromatography and LC-MS analysis. However, it appeared that the degree of dimethylarginine formation was quite different when analyzed by these two methods. In our studies with *Tb*PRMT7, the homologous mutation, M75F, showed no change in PRMT7's type III activity with substrates, including RBP16 (25) and the H4(1–21) R3MMA peptide (Table 1). To validate the PRMT1 mutant activity (24), we compared the product specificity of the wild-type human PRMT1 (Fig. 6*A*) with the H4(1–21) and H4(1–21) R3MMA peptides to that of the rat PRMT1 M48F enzyme (Fig. 6*B*). We chose these peptides because H4(1–21) has been shown to be a robust PRMT1 substrate (31, 32). However, in contrast to the earlier work (24), we were unable to distinguish any difference in the product specificity of the wild-type human PRMT1 and the rat PRMT1 M48F mutant with the H4 peptide substrates using high resolution cation exchange chromatography (Fig. 6). With both enzymes, only MMA and ADMA were formed under conditions where we could detect SDMA at a level of less than 0.4% of

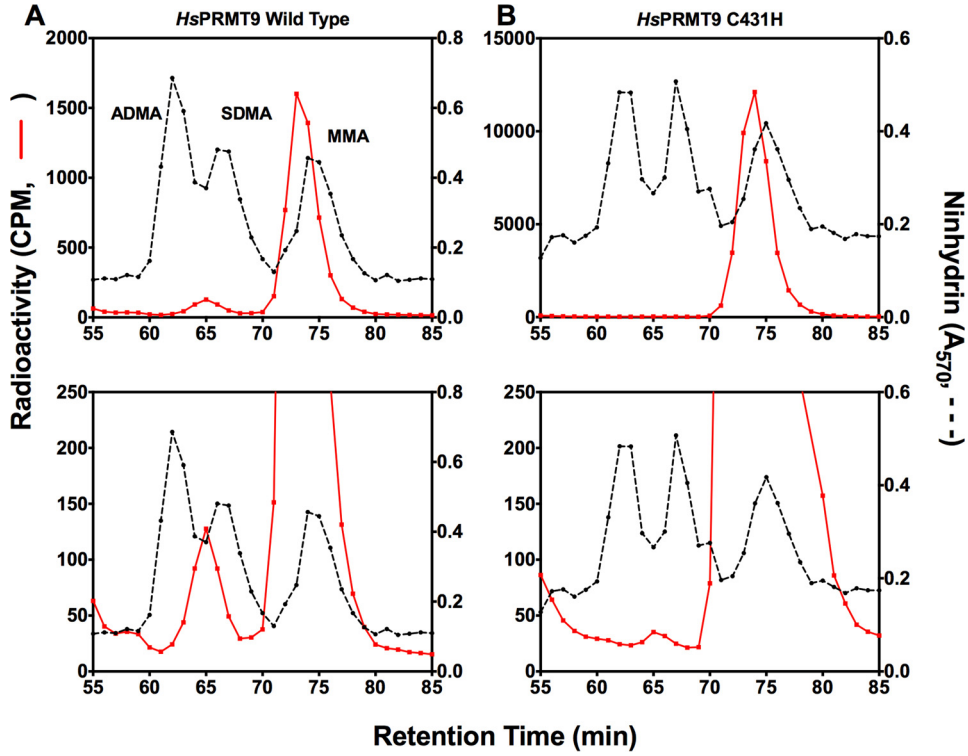

FIGURE 5. ***Hs*PRMT9 C431H mutant displays diminished SDMA and greatly increased MMA production with GST-SF3B2.** *A,* amino acid analysis of methylated arginine derivatives produced by the wild-type human GST-PRMT9 (*Hs*PRMT9) with substrate GST-SF3B2 as described under "Experimental Procedures." *B,* amino acid analysis of methylated arginine derivatives produced by the C431H mutant human GST-PRMT9 with substrate GST-SF3B2. In each case, the *lower panels* represent enlargement of the radioactivity in the *upper panels* to show low levels of methylation. As given under the "Experimental Procedures," 86 cpm correspond to 1 fmol of methyl groups. This experiment is one of two biological replicates.

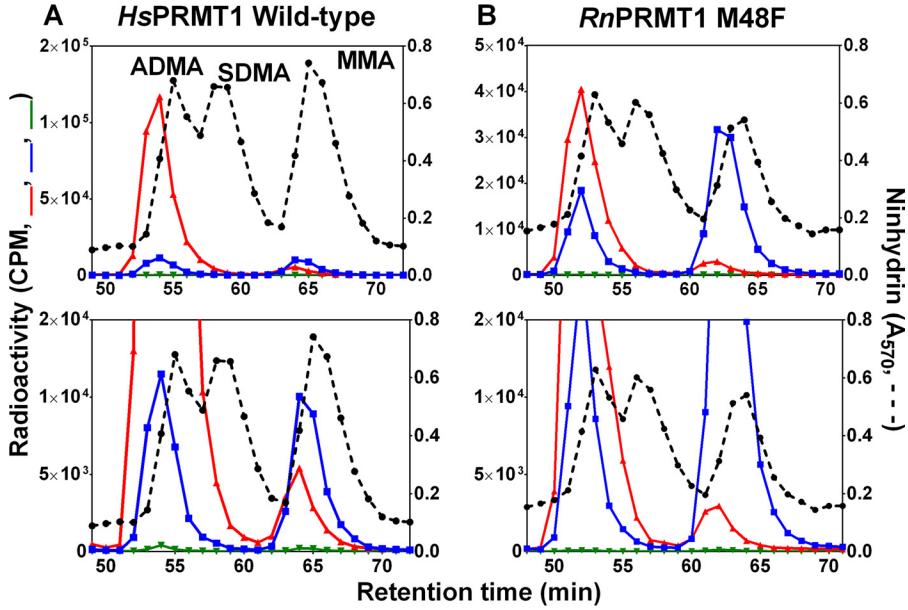

FIGURE 6. ***Rn*PRMT1 M48F mutant enzyme does not produce SDMA with histone H4 peptides.** *In vitro* methylation and cation exchange chromatography were used as described under the "Experimental Procedures" to assess PRMT1 activity and product specificity with H4(1–21) (*blue*), H4(1–21) R3MMA (*red*), and the enzyme alone (*green*). *Dashed black lines* indicate elution profile of non-radioactive methylarginine species as measured by a ninhydrin assay (see "Experimental Procedures"). *A,* amino acid analysis of methylated arginine derivatives produced by human PRMT1 (*Hs*PRMT1). *B,* amino acid analysis of methylated arginine derivatives produced by rat PRMT1 (*Rn*PRMT1) M48F mutant. In each case, the *lower panels* represent enlargement of the radioactivity in the *upper panels* to show low levels of methylation. As given under the "Experimental Procedures," 86 cpm correspond to 1 fmol of methyl groups. This experiment represents one of two biological replicates.

the radioactivity in ADMA. Significantly, in the presence of an already methylated substrate such as H4(1–21) R3MMA, the rat PRMT1 M48F was still unable to produce any SDMA (Fig. 6*B*). Additionally, there is MMA production above automethylation levels for wild-type human PRMT1 and rat PRMT1 M48F when given H4(1–21) R3MMA as a substrate. The MMA

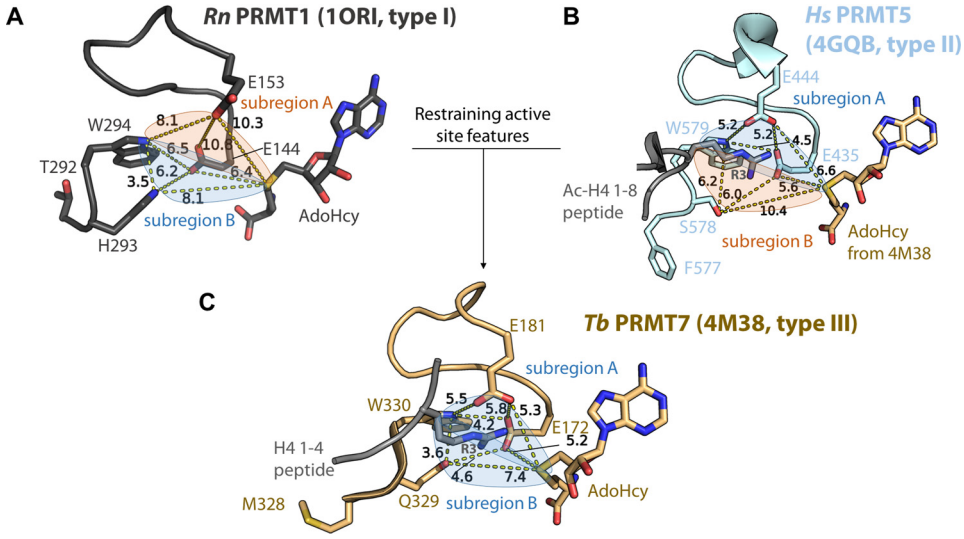

FIGURE 7. **PRMT active sites display distinct spatial architectures.** The active site (double E loop, THW loop, and AdoHcy) from *Rn*PRMT1 (1ORI, chain A; *dark gray*) (*A*), *Hs*PRMT5 (4GQB, chain A; *cyan*) (*B*), and *Tb*PRMT7 (4M38, chain A; *wheat*) (*C*) are shown. Crowded subregions of the active sites are highlighted in *light blue* and open subregions are highlighted in *orange*. *B* and *C*, substrate peptides co-crystallized with the enzyme are also shown. Distances between atoms are given in Ångströms and indicated by *yellow dashed lines*. Images were made using PyMOL (Schrödinger, LLC).

being produced with this peptide would be expected to occur at positions Arg-17 and Arg-19. These results indicate that the residue Met-48 may not be involved in mediating product specificity in mammalian PRMT1.

Discussion

Different methylarginine marks can be recognized by distinct reader proteins (17) and often behave as epigenetic switches, affecting the activation or silencing of certain genes (15, 16). Given the significance of ADMA and SDMA marks, it has become increasingly important to understand how product specificity arises to generate these residues. Having previously demonstrated the conversion of *Tb*PRMT7, a strictly MMA-producing type III enzyme, into a type I enzyme forming ADMA by mutation (25), we now present another *Tb*PRMT7 mutant that is capable of producing SDMA, exhibiting the product specificity of type II PRMTs (Fig. 2). Biochemical and mutational analyses of the enzyme's catalytic activity reveal that SDMA production occurs when it is presented with an already monomethylated substrate, demonstrating that this mutant of PRMT7, in contrast to the wild type, is able to recognize a monomethylated molecule as a substrate and carry out further methylation. In fact, the E181D/Q329A mutant enzyme binds H4(1–21) R3MMA with a higher affinity than the corresponding unmethylated peptide (Fig. 4). This observation illustrates that although the activity of the E181D/Q329A mutant is low, it still behaves, on the catalytic level, as a type II PRMT.

We also examined a mammalian PRMT1 mutant enzyme that was previously reported to produce SDMA along with its wild-type products, ADMA and MMA (24). We were unable to observe any symmetric dimethylation on histone H4 peptide substrates from this rat PRMT1 mutant enzyme (M48F) (Fig. 6). Coupled with our results from amino acid analysis of a homologous mutation in *Tb*PRMT7 (M75F; Table 1) and its mutation to alanine (M75A; Table 1) (25), our work did not confirm any role of Met-48 in affecting PRMT1 product specificity in the mammalian enzyme. It should be noted that the H4 peptide substrates used in our study differ from the GGRGGFGGRGGFGGRGGFG peptide used previously (24). Additionally, immunoblot analysis revealed that the reverse mutation in the PRMT5 enzymes of humans and *Caenorhabditis elegans*, where the corresponding wild-type residue is a phenylalanine (F327M and F379M, respectively) caused asymmetric dimethylation of human histone H4 (14). It would be interesting to examine these mutants with our more sensitive amino acid analysis techniques to determine any changes in product specificity more precisely.

Our previous mutagenesis results (25), coupled with those discussed here, highlight the major features of the PRMT active site, which may control mono- and dimethylation specificity. Conceptually, the active site of PRMTs, defined by the double E loop, the THW loop, and the AdoMet/AdoHcy cofactor, can be divided into two subregions, one of which is located between the two glutamate residues of the double E loop and above the substrate arginine (subregion A), while subregion B is adjacent to the THW loop and the region underneath the substrate arginine as displayed in Fig. 7. Our analysis reveals that the nature of these two subregions correlates well with, and therefore seems predictive of, product specificity in PRMTs. Specifically, type I PRMTs contain an open subregion A and a spatially restricted subregion B (Fig. 7*A*). The nature of these subregions in type II active sites is reversed with respect to type I PRMTs, with an open subregion B and a restricted subregion A (Fig. 7*B*). PRMT7's active site by contrast contains two restricted subregions, combining the restraining features of subregions A (type I) and B (type II) of the other two types of PRMTs (Fig. 7*C*). These spatial restrictions may be the key for PRMT7 to only monomethylate its substrates, thus classifying it as a type III PRMT enzyme.

The E181D mutation of *Tb*PRMT7 increases the space within subregion A of the active site by a single carbon-carbon

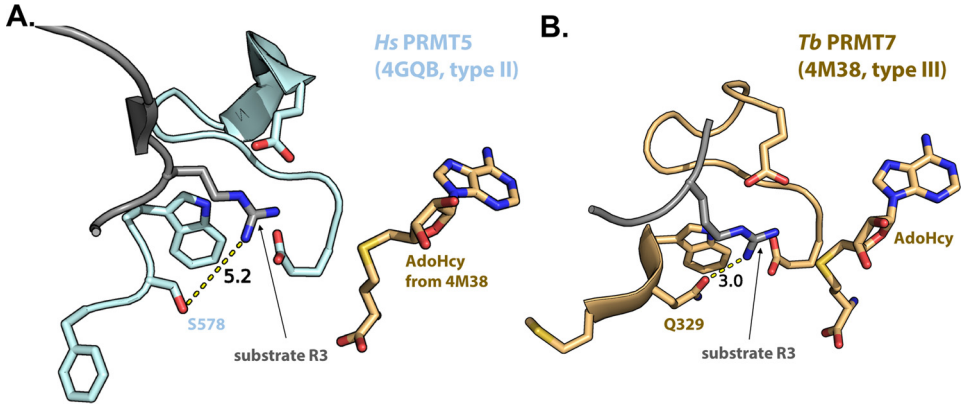

FIGURE 8. **THW loop of PRMT5 is further away from the substrate arginine than the THW loop of PRMT7.** *A,* active site of human PRMT5 (4GQB) is shown. *B,* active site of *Tb*PRMT7 (4M38) is shown. Distances between atoms are given in Ångströms and indicated by *yellow dashed lines*.

bond where the substrate arginine is stabilized. The distance between the glutamates of the double E loop, however, is not the essential factor in SDMA production because the glutamates of human PRMT5, the major SDMA producer in the cell, are actually closer together than even those in *Tb*PRMT7 (Fig. 7, *B* and *C*). The methylation type alteration can be largely attributed to the Q329A mutation, which, in combination with E181D, may result in the opening up of subregion B in the active site underneath the substrate arginine. It is important to note that the Q329A single mutant did not produce SDMA, suggesting that the THW loop may not be the sole contributor in determining type II methylation. Human PRMT5 has a serine residue in place of the corresponding glutamine residue in *Tb*PRMT7 that is located at a greater distance (5.2 Å *versus* 3.0 Å; Fig. 8) from the substrate arginine than the glutamine of *Tb*PRMT7 and is also pointed away from the active site (Fig. 7). In our *Tb*PRMT7 E181D/Q329A construct, the glutamine to alanine substitution removes an acetamide moiety in subregion B. This active-site alteration now allows for methylated arginines to bind more favorably and is better suited to accommodate a methylated nitrogen atom near the THW loop, allowing the other terminal nitrogen atom (positioned near the double E loop) to become methylated. A specific role of the THW loop in determining PRMT product specificity was first suggested in two recent reviews from Thompson and co-workers (2, 20).

In support of the importance of the THW loop in determining type II PRMT product specificity, the mutation of C431H in human PRMT9 shows a significant decrease in SDMA production relative to the wild-type enzyme (Fig. 5). Although no structure has been determined for this enzyme, the cysteine to histidine mutation introduces a bulkier moiety into the THW loop potentially contributing to further crowding in the active site, which in turn may prevent SDMA production. The concomitant marked increase in MMA production of the PRMT9 is consistent with a partially processive methylation mechanism, a characteristic of type I PRMTs (33).

Structural alignments of known type I, II, and III PRMTs show that the geometries of the active sites are highly conserved within each PRMT type (Fig. 9 and Table 2). Although our proposed model will benefit from further validation through structural studies of novel PRMTs and additional mutant enzymes, our results illustrate how small changes in the active site of PRMTs can markedly alter their catalytic specificity and thus aid in creating a spectrum of methylarginine species that may differentially mediate various biological pathways.

The emerging role of PRMTs in cancer (4, 5, 34, 35) has profoundly spurred the research into PRMT inhibitors (36). One of the major issues in this field, however, has been the promiscuity of many PRMT inhibitors derived from small molecule library screening (37). Approaches based on finding bisubstrate analogs that mimic the cofactor and the substrate arginine have the disadvantages of promiscuity and additionally, due to their highly charged nature, limited bioavailability precluding their administration as oral drugs (37). In light of such obstacles in the development of small molecule inhibitors of PRMTs involved in various diseases, it is our hope that our model will facilitate the rational design of specific and potent PRMT inhibitors by providing detailed insight into the distinct active-site architectures of the three types of PRMTs.

Experimental Procedures

Peptide Substrates—Histone H4(1–21) (Ac-SGRGKGGK-GLGKGGAKRHRKV) and histone H4(1–21) R3MMA (Ac-SGR(me)GKGGKGLGKGGAKRHRKV) peptides were kind gifts from Heather Rust (The Scripps Research Institute, Jupiter, FL) and Paul Thompson (University of Massachusetts Medical School, Worcester, MA). Peptides used for ITC analysis were purchased from AnaSpec.

Protein Expression and Purification—*Tb*PRMT7 wild-type and mutant enzymes were cloned, expressed, and purified as described previously (25). GST-PRMT9 wild-type, GST-PRMT9 C431H mutant, and GST-SF3B2(401–550) fragment were expressed and purified as described previously (28).

Human PRMT1 (*Hs*PRMT1) was expressed from a pET28b(+) vector with a short N-terminal His tag obtained from Dr. Paul Thompson (University of Massachusetts Medical School, Worcester, MA) (38). Rat PRMT1 (*Rn*PRMT1) M48F was expressed from a pET28b(+) vector obtained from Dr. Joan Hevel (Utah State University, Logan, UT) (24). Both constructs were expressed in *Escherichia coli* BL21(DE3) cells (Invitrogen) and grown in LB media con-

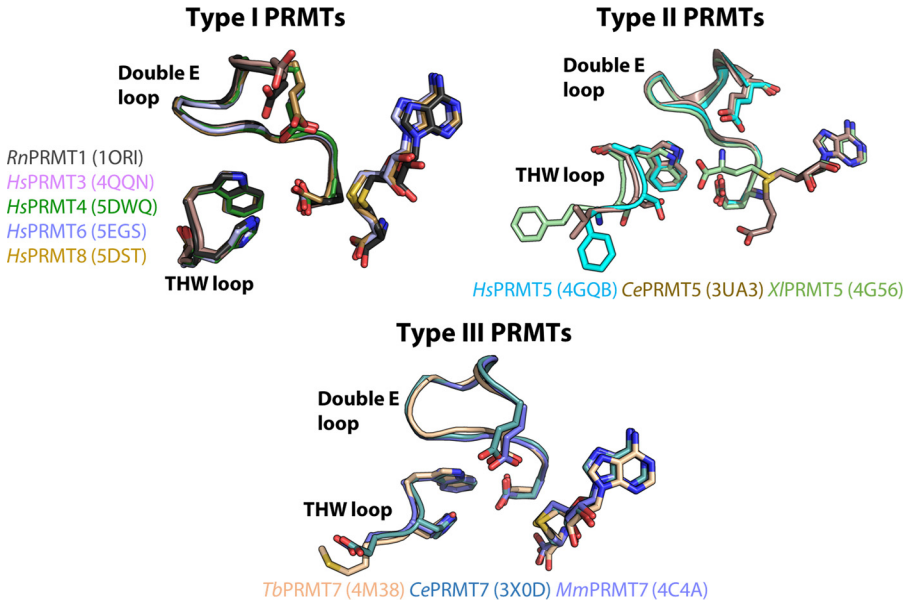

FIGURE 9. **Structural alignment of PRMT active sites.** Active sites of all three types of PRMTs are shown.

TABLE 2

Root mean square deviation (r.m.s.d.) values for structural alignments of the active-site double E loop, the THW loop, and AdoHcy made in PyMOL for type I, II, and III PRMTs from the indicated crystal structures

	PRMTs	r.m.s.d. (Å)	
		Cα	All atoms
Type I			
	*Rn*PRMT1 (1ORI)	0	0
	*Hs*PRMT3 (4QQN)	0.5	1.2
	*Hs*PRMT4 (5DWQ)	0.6	1.3
	*Hs*PRMT6 (5EGS)	0.7	1.2
	*Hs*PRMT8 (5DST)	0.6	1.1
Type II			
	*Hs*PRMT5 (4GQB)	0	0
	*Ce*PRMT5 (3UA3)	0.3	0.6
	*Xl*PRMT5 (4G56)	0.4	1.6
Type III			
	*Tb*PRMT7 (4M38)	0	0
	*Ce*PRMT7 (3X0D)	0.7	1.0
	*Mm*PRMT7 (4C4A)	0.7	1.1

taining kanamycin at 37 °C to an OD_{600} of ~0.6. Expression was induced with 1 mM isopropyl β-D-thiogalactoside (GoldBio) at 18 °C for 16 h. The cells were then harvested by centrifugation at 5,000 × *g* and 4 °C. The harvested cells were lysed using an EmulsiFlex cell homogenizer (Avestin) in 50 mM HEPES (pH 8.0), 300 mM NaCl, 0.5 mM phenylmethylsulfonyl fluoride (Sigma), and complete EDTA-free protease inhibitor mixture (Pierce). Lysed cells were centrifuged at 15,000 rpm for 50 min at 4 °C. The clarified lysate was loaded onto a 5-ml HisTrap HP Ni^{2+} column (GE Healthcare). The column was washed with 10 column volumes of the lysis buffer, including 50 mM imidazole-HCl (pH 8.0), and the protein was eluted with a 50–500 mM imidazole-HCl (pH 8.0) gradient. The eluted protein's purity was verified through SDS-PAGE analysis to be >95% (~40.6 kDa). The protein was then dialyzed against a storage buffer containing 50 mM HEPES (pH 8.0), 1 mM DTT, and 15% glycerol (v/v).

Isothermal Titration Calorimetry—ITC measurements were performed at 15 °C using a MicroCal auto-iTC200 calorimeter (MicroCal, LLC). Protein was incubated with 2-fold molar excess of AdoHcy for 1 h at room temperature. Protein and peptide samples were then extensively dialyzed against a buffer containing 20 mM HEPES (pH 7.5), 20 mM NaCl, and 0.5 mM tris(2-carboxyethyl)phosphine. 2 μl of 1–4 mM peptide was injected into 0.2 ml of 0.1–0.4 mM protein in the chamber every 150 s. Baseline-corrected data were analyzed with ORIGIN software.

Amino Acid Analysis of Protein and Peptide Substrates—*In vitro* methylation assays and amino acid analysis using the *Tb*PRMT7 wild-type and mutant enzymes were performed as described previously (25) in a buffer of 50 mM HEPES (pH 8.0), 10 mM NaCl, 1 mM DTT, and 5% glycerol in a final volume of 60 μl. Assays and amino acid analysis using human PRMT9 were also carried out as described previously (28, 29). For methylation assays with PRMT1, human and rat enzymes were used. The wild-type control was done with human PRMT1, and the mutant reactions were done with rat PRMT1 M48F. In both cases, 2.5 μg of PRMT1 and either 50 μM H4(1–21) or H4(1–21) R3MMA peptide were incubated at 37 °C for 3 h in a mixture containing 0.7 μM of *S*-adenosyl-L-[*methyl*-^{3}H]methionine ([*methyl*-^{3}H]AdoMet) (PerkinElmer Life Sciences; stock solution of 7 μM (78.2 Ci/mmol) in 10 mM H_2SO_4/EtOH (9:1, v/v)), 50 mM HEPES (pH 8.0), 10 mM NaCl, 1 mM DTT, and 5% glycerol in a final volume of 60 μl. Reactions were stopped, acid-hydrolyzed, and analyzed with cation exchange chromatography as described previously (25). Given the specific radioactivity of the [*methyl*-^{3}H]-AdoMet of 78.2 Ci/mmol and a counting efficiency of 50%, 1 fmol of methyl groups corresponds to 86 cpm.

Author Contributions—K. J., R. A. W., E. W. D., A. H., P. S., and S. G. C. planned the experiments. Experiments were performed by K. J., R. A. W., E. W. D., and A. H. K. J. and R. A. W. drafted the manuscript. K. J., R. A. W., E. W. D., A. H., P. S., and S. G. C. participated in the data analysis and interpretation, and K. J., R. A. W., E. W. D., A. H., P. S., and S. G. C. participated in manuscript revisions.

Acknowledgments—We thank H. Rust (The Scripps Research Institute) and P. Thompson (University of Massachusetts Medical School) for providing the H4(1–21) and H4(1–21) R3MMA peptides and the human His-PRMT1 plasmid; J. Hevel (Utah State University, Logan, UT) for providing the rat His-PRMT1 M48F plasmid; M. Dzialo (University of Leuven, Belgium) for help with amino acid analysis; G. Blobel (Rockefeller University) for support; D. Berman (Rockefeller University) for help with protein expression and purification; D. King (University of California at Berkeley) for mass spectrometry analysis; and the High Throughput Screening and Spectroscopy Resource Center at Rockefeller University.

References

1. Walsh, G., and Jefferis, R. (2006) Post-translational modifications in the context of therapeutic proteins. *Nat. Biotechnol.* **24,** 1241–1252
2. Fuhrmann, J., Clancy, K. W., and Thompson, P. R. (2015) Chemical biology of protein arginine modifications in epigenetic regulation. *Chem. Rev.* **115,** 5413–5461
3. Morales, Y., Cáceres, T., May, K., and Hevel, J. M. (2016) Biochemistry and regulation of the protein arginine methyltransferases (PRMTs). *Arch. Biochem. Biophys.* **590,** 138–152
4. Baldwin, R. M., Haghandish, N., Daneshmand, M., Amin, S., Paris, G., Falls, T. J., Bell, J. C., Islam, S., and Côté, J. (2015) Protein arginine methyltransferase 7 promotes breast cancer cell invasion through the induction of MMP9 expression. *Oncotarget.* **6,** 3013–3032
5. Yao, R., Jiang, H., Ma, Y., Wang, L., Wang, L., Du, J., Hou, P., Gao, Y., Zhao, L., Wang, G., Zhang, Y., Liu, D.-X., Huang, B., and Lu, J. (2014) PRMT7 induces epithelial-to-mesenchymal transition and promotes metastasis in breast cancer. *Cancer Res.* **74,** 5656–5667
6. Yang, Y., and Bedford, M. T. (2013) Protein arginine methyltransferases and cancer. *Nat. Rev. Cancer* **13,** 37–50
7. Karkhanis, V., Wang, L., Tae, S., Hu, Y. J., Imbalzano, A. N., and Sif, S. (2012) Protein arginine methyltransferase 7 regulates cellular response to DNA damage by methylating promoter histones H2A and H4 of the polymerase δ catalytic subunit gene, POLD1. *J. Biol. Chem.* **287,** 29801–29814
8. Wang, Y.-C., Peterson, S. E., and Loring, J. F. (2014) Protein post-translational modifications and regulation of pluripotency in human stem cells. *Cell Res.* **24,** 143–160
9. Lott, K., Zhu, L., Fisk, J. C., Tomasello, D. L., and Read, L. K. (2014) Functional interplay between protein arginine methyltransferases in *Trypanosoma brucei*. *Microbiologyopen* **3,** 595–609
10. Ferreira, T. R., Alves-Ferreira, E. V., Defina, T. P., Walrad, P., Papadopoulou, B., and Cruz, A. K. (2014) Altered expression of an RBP-associated arginine methyltransferase 7 in *Leishmania major* affects parasite infection. *Mol. Microbiol.* **94,** 1085–1102
11. Bedford, M. T., and Clarke, S. G. (2009) Protein arginine methylation in mammals: who, what, and why. *Mol. Cell* **33,** 1–13
12. Martens-Lobenhoffer, J., Bode-Böger, S. M., and Clement, B. (2016) First detection and quantification of *N*(δ)-monomethylarginine, a structural isomer of *N* (G)-monomethylarginine, in humans using MS(3). *Anal. Biochem.* **493,** 14–20
13. Wang, H., Huang, Z. Q., Xia, L., Feng, Q., Erdjument-Bromage, H., Strahl, B. D., Briggs, S. D., Allis, C. D., Wong, J., Tempst, P., and Zhang, Y. (2001) Methylation of histone H4 at arginine 3 facilitating transcriptional activation by nuclear hormone receptor. *Science* **293,** 853–857
14. Sun, L., Wang, M., Lv, Z., Yang, N., Liu, Y., Bao, S., Gong, W., and Xu, R.-M. (2011) Structural insights into protein arginine symmetric dimethylation by PRMT5. *Proc. Natl. Acad. Sci.* **108,** 20538–20543
15. Dhar, S. S., Lee, S.-H., Kan, P.-Y., Voigt, P., Ma, L., Shi, X., Reinberg, D., and Lee, M. G. (2012) Trans-tail regulation of MLL4-catalyzed H3K4 methylation by H4R3 symmetric dimethylation is mediated by a tandem PHD of MLL4. *Genes Dev.* **26,** 2749–2762
16. Migliori, V., Müller, J., Phalke, S., Low, D., Bezzi, M., Mok, W. C., Sahu, S. K., Gunaratne, J., Capasso, P., Bassi, C., Cecatiello, V., De Marco, A., Blackstock, W., Kuznetsov, V., Amati, B., *et al.* (2012) Symmetric dimethylation of H3R2 is a newly identified histone mark that supports euchromatin maintenance. *Nat. Struct. Mol. Biol.* **19,** 136–144
17. Gayatri, S., and Bedford, M. T. (2014) Readers of histone methylarginine marks. *Biochim. Biophys. Acta* **1839,** 702–710
18. Suárez-Calvet, M., Neumann, M., Arzberger, T., Abou-Ajram, C., Funk, E., Hartmann, H., Edbauer, D., Kremmer, E., Göbl, C., Resch, M., Bourgeois, B., Madl, T., Reber, S., Jutzi, D., Ruepp, M.-D., *et al.* (2016) Monomethylated and unmethylated FUS exhibit increased binding to Transportin and distinguish FTLD-FUS from ALS-FUS. *Acta Neuropathol.* **131,** 587–604
19. Dhar, S., Vemulapalli, V., Patananan, A. N., Huang, G. L., Di Lorenzo, A., Richard, S., Comb, M. J., Guo, A., Clarke, S. G., and Bedford, M. T. (2013) Loss of the major type I arginine methyltransferase PRMT1 causes substrate scavenging by other PRMTs. *Sci. Rep.* **3,** 1311
20. Fuhrmann, J., and Thompson, P. R. (2016) Protein arginine methylation and citrullination in epigenetic regulation. *ACS Chem. Biol.* **11,** 654–668
21. Schapira, M., and Ferreira de Freitas, R. (2014) Structural biology and chemistry of protein arginine methyltransferases. *Medchemcomm* **5,** 1779–1788
22. Cura, V., Troffer-Charlier, N., Wurtz, J. M., Bonnefond, L., and Cavarelli, J. (2014) Structural insight into arginine methylation by the mouse protein arginine methyltransferase 7: a zinc finger freezes the mimic of the dimeric state into a single active site. *Acta Crystallogr. D Biol. Crystallogr* **70,** 2401–2412
23. Hasegawa, M., Toma-Fukai, S., Kim, J. D., Fukamizu, A., and Shimizu, T. (2014) Protein arginine methyltransferase 7 has a novel homodimer-like structure formed by tandem repeats. *FEBS Lett.* **588,** 1942–1948
24. Gui, S., Gathiaka, S., Li, J., Qu, J., Acevedo, O., and Hevel, J. M. (2014) A remodeled protein arginine methyltransferase 1 (PRMT1) generates symmetric dimethylarginine. *J. Biol. Chem.* **289,** 9320–9327
25. Debler, E. W., Jain, K., Warmack, R. A., Feng, Y., Clarke, S. G., Blobel, G., and Stavropoulos, P. (2016) A glutamate/aspartate switch controls product specificity in a protein arginine methyltransferase. *Proc. Natl. Acad. Sci. U.S.A.* **113,** 2068–2073
26. Fisk, J. C., Sayegh, J., Zurita-Lopez, C., Menon, S., Presnyak, V., Clarke, S. G., and Read, L. K. (2009) A type III protein arginine methyltransferase from the protozoan parasite *Trypanosoma brucei*. *J. Biol. Chem.* **284,** 11590–11600
27. Wang, C., Zhu, Y., Caceres, T. B., Liu, L., Peng, J., Wang, J., Chen, J., Chen, X., Zhang, Z., Zuo, X., Gong, Q., Teng, M., Hevel, J. M., Wu, J., and Shi, Y. (2014) Structural determinants for the strict monomethylation activity by *Trypanosoma brucei* protein arginine methyltransferase 7. *Structure* **22,** 756–768
28. Hadjikyriacou, A., Yang, Y., Espejo, A., Bedford, M. T., and Clarke, S. G. (2015) Unique features of human protein arginine methyltransferase 9 (PRMT9) and its substrate RNA splicing factor SF3B2. *J. Biol. Chem.* **290,** 16723–16743
29. Yang, Y., Hadjikyriacou, A., Xia, Z., Gayatri, S., Kim, D., Zurita-Lopez, C., Kelly, R., Guo, A., Li, W., Clarke, S. G., and Bedford, M. T. (2015) PRMT9 is a type II methyltransferase that methylates the splicing factor SAP145. *Nat. Commun.* **6,** 6428
30. Feng, Y., Maity, R., Whitelegge, J. P., Hadjikyriacou, A., Li, Z., Zurita-Lopez, C., Al-Hadid, Q., Clark, A. T., Bedford, M. T., Masson, J. Y., and Clarke, S. G. (2013) Mammalian protein arginine methyltransferase 7 (PRMT7) specifically targets RXR sites in lysine- and arginine-rich regions. *J. Biol. Chem.* **288,** 37010–37025
31. Feng, Y., Xie, N., Jin, M., Stahley, M. R., Stivers, J. T., and Zheng, Y. G. (2011) A transient kinetic analysis of PRMT1 catalysis. *Biochemistry* **50,** 7033–7044
32. Huang, S., Litt, M., and Felsenfeld, G. (2005) Methylation of histone H4 by arginine methyltransferase PRMT1 is essential in vivo for many subsequent histone modifications. *Genes Dev.* **19,** 1885–1893
33. Wang, M., Xu, R.-M., and Thompson, P. R. (2013) Substrate specificity, processivity, and kinetic mechanism of protein arginine methyltransferase 5. *Biochemistry* **52,** 5430–5440
34. Bao, X., Zhao, S., Liu, T., Liu, Y., Liu, Y., and Yang, X. (2013) Overexpression of PRMT5 promotes tumor cell growth and is associated with poor

disease prognosis in epithelial ovarian cancer. *J. Histochem. Cytochem.* **61,** 206–217
35. Tarighat, S. S., Santhanam, R., Frankhouser, D., Radomska, H. S., Lai, H., Anghelina, M., Wang, H., Huang, X., Alinari, L., Walker, A., Caligiuri, M. A., Croce, C. M., Li, L., Garzon, R., Li, C., *et al.* (2016) The dual epigenetic role of PRMT5 in acute myeloid leukemia: gene activation and repression via histone arginine methylation. *Leukemia* **30,** 789–799
36. Schapira, M., and Arrowsmith, C. H. (2016) Methyltransferase inhibitors for modulation of the epigenome and beyond. *Curr. Opin. Chem. Biol.* **33,** 81–87
37. Hu, H., Qian, K., Ho, M.-C., and Zheng, Y. G. (2016) Small molecule inhibitors of protein arginine methyltransferases. *Expert Opin. Investig. Drugs.* **25,** 335–358
38. Zhang, X., and Cheng, X. (2003) Structure of the predominant protein arginine methyltransferase PRMT1 and analysis of its binding to substrate peptides. *Structure* **11,** 509–520
39. Zurita-Lopez, C. I., Sandberg, T., Kelly, R., and Clarke, S. G. (2012) Human protein arginine methyltransferase 7 (PRMT7) is a type III enzyme forming ω-N^G-monomethylated arginine residues. *J. Biol. Chem.* **287,** 7859–7870
40. Gottschling, H., and Freese, E. (1962) A tritium isotope effect on ion exchange chromatography. *Nature* **196,** 829–831

Protein Arginine Methyltransferase Product Specificity Is Mediated by Distinct Active-site Architectures

Kanishk Jain, Rebeccah A. Warmack, Erik W. Debler, Andrea Hadjikyriacou, Peter Stavropoulos and Steven G. Clarke

J. Biol. Chem. 2016, 291:18299-18308.
doi: 10.1074/jbc.M116.740399 originally published online July 7, 2016